University of Nebraska - Lincoln
DigitalCommons@University of Nebraska - Lincoln

Conservation and Survey Division | Natural Resources, School of

2-19-2024

Analysis of legacy gravity data reveals sediment-filled troughs buried under Flathead Valley, Montana, USA

Ali Gebril

Mohamed A. Khalil

Robert Matthew Joeckel

James Rose

Follow this and additional works at: https://digitalcommons.unl.edu/conservationsurvey

 Part of the Geology Commons, Geomorphology Commons, Hydrology Commons, Paleontology Commons, Sedimentology Commons, Soil Science Commons, and the Stratigraphy Commons

This Article is brought to you for free and open access by the Natural Resources, School of at DigitalCommons@University of Nebraska - Lincoln. It has been accepted for inclusion in Conservation and Survey Division by an authorized administrator of DigitalCommons@University of Nebraska - Lincoln.

Check for updates

Received: 9 June 2023 | Accepted: 19 February 2024

DOI: 10.1002/nsg.12295

Near Surface Geophysics | EAGE European Association of Geoscientists & Engineers

ORIGINAL ARTICLE

Analysis of legacy gravity data reveals sediment-filled troughs buried under Flathead Valley, Montana, USA

Ali Gebril[1] | **Mohamed A. Khalil**[2] | **R. M. Joeckel**[2] | **James Rose**[3]

[1]Groundwater Investigation Program, Montana Bureau of Mines and Geology, Butte, Montana, USA

[2]Conservation and Survey Division, School of Natural Resources, University of Nebraska-Lincoln, Lincoln, Nebraska, USA

[3]Water and Environmental Technologies, Butte, Montana, USA

Correspondence
Mohamed A. Khalil, Conservation and Survey Division, School of Natural Resources, University of Nebraska-Lincoln, Lincoln, NE 68583-0961, USA. Email: maboushanab2@unl.edu.

Abstract

Shallow, dominantly silt- and clay-filled erosional troughs in Quaternary sediments under the Flathead Valley (northwestern Montana, USA) are very likely to be hydraulic barriers limiting the horizontal flow of groundwater. Accurately mapping them is important because of increasing demand for groundwater. We used a legacy Bouguer gravity map measured in 1968. The directional derivatives of the map are computed, and the map was enhanced by implementing edge detection tools. We produced generalized derivative, maximum horizontal gradient, total gradient and tilt gradient maps through two-dimensional Fourier transform analysis. These maps were remarkably successful in locating buried troughs in the northern and northwestern parts of the study area, closely matching locations determined previously from compiled borehole data. Our results also identify hitherto unknown extensions of troughs and indicate that some of the buried troughs may be connected.

KEYWORDS

gravity, groundwater, legacy data, near surface, potential field filtering, troughs

INTRODUCTION

The Flathead Valley is a 90 km-long, 809 km^2, intermontane basin associated with a recently active half graben (Stickney et al., 2000, Smith, 2004b) in the Rocky Mountains of northwestern Montana (Figure 1). The Flathead Valley is bordered by the Swan Range in the eastern and northeastern directions and the Whitefish Mountains in the northern directions (Figure 1). The valley contains Flathead Lake, the largest natural freshwater lake in the contiguous western USA and a remnant of the latest Pleistocene glacial Lake Missoula. Valley floor elevation ranges from about 884 metres above sea level (MASL), where the Flathead River enters Flathead Lake, to 945 MASL at the margins of the valley (Rose, 2018). More than 45,000 people live in the valley communities of Kalispell, Bigfork, Columbia Falls and Whitefish, Montana. Flathead County (population >111,000), in which most of the valley lies, has nearly doubled in population since 1990 to be the fourth most populous of Montana's 56 counties (U.S. Census Bureau, July 1, 2022). Concomitantly, municipal, domestic and irrigation demands on groundwater resources have increased markedly (U.S. Environmental Protection Agency, 2011). These pressures, in the context of the complexity of basin-fill stratigraphy and groundwater flow systems within the Flathead Valley (LaFave et al., 2004; LaFave, 2004; Smith, 2004b) need a more comprehensive understanding of local geology and hydrogeology, to which geophysical studies such as ours include important insights.

Buried, sediment-filled troughs under the Flathead Valley are thought to be products of subglacial or outwash-stream erosion in the late Pleistocene (John LaFave, Montana Bureau of Mines and Geology, personal communication, June 2, 2023). These troughs are very likely to play a major role in regional hydrostratigraphy by acting as hydraulic barriers, slowing the lateral

This is an open access article under the terms of the Creative Commons Attribution-NonCommercial-NoDerivs License, which permits use and distribution in any medium, provided the original work is properly cited, the use is non-commercial and no modifications or adaptations are made.
© 2024 The Authors. *Near Surface Geophysics* published by John Wiley & Sons Ltd on behalf of European Association of Geoscientists and Engineers.

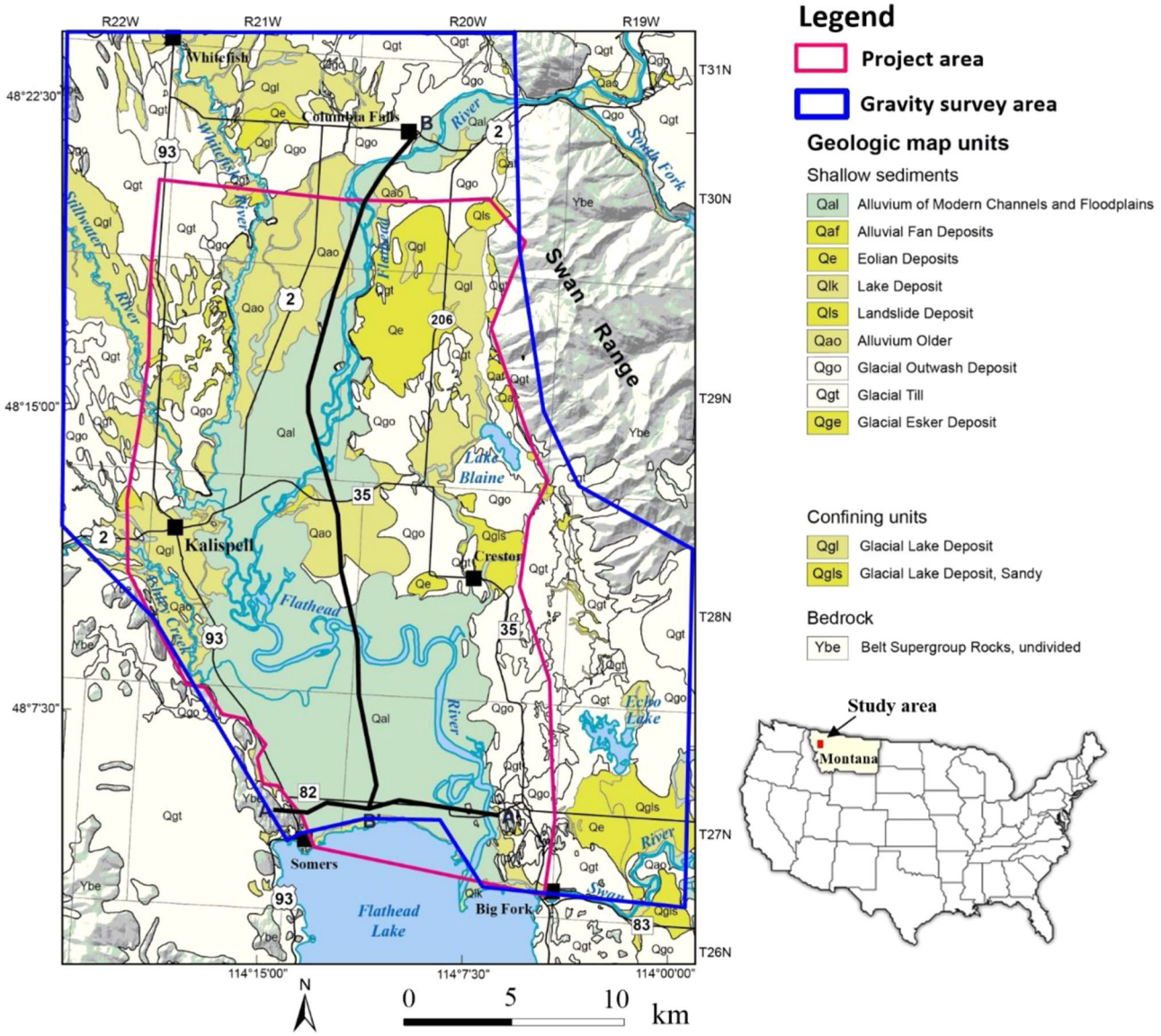

Figure 1 Surficial geology map of the Flathead Valley shows the gravity survey area. The study area is dominated by Quaternary glacial and alluvial deposits on the floor of the Flathead Valley and the Mesoproterozoic Belt Supergroup in the surrounding highlands, modified from Smith (2004a) (from Rose, 2018; reproduced with permission from the Montana Bureau of Mines and Geology). The inset map at the lower right shows the location of Montana and the study area within the contiguous United States.

flow of groundwater from highly conductive zones. Prior to the present study, the sediment-filled troughs in the Flathead Valley were known only from the interpretation of borehole data. The gravity data we detail in this paper provide a means by which the sediment-filled troughs can be mapped continuously and in greater detail than before. Indeed, gravity methods have recently proven efficacious in addressing sedimentological and hydrogeological problems (e.g., Amiri et al., 2011, Barhoumit et al., 2021; Khalil et al., 2014, 2015, Khalil & Santos 2015b; Xue et al., 2022). As a point of clarification, we observe that the term 'trough' is frequently used in North America to describe depressions eroded into bedrock and commonly in cases of glacial erosion. Nevertheless, the term is equally valid for application to elongate depressions eroded in sediments. Furthermore, we emphasize that the Flathead Valley, like related features in the enclosing region, has a complex Cenozoic history that includes not only glacial and fluvial erosion and deposition, but also the creation of the valley itself by extensional tectonics and multiple phases of fault movement (McMechan & Price, 1980; Constenius, 1996; Hofmann et al., 2006).

Flathead Valley experiences more stable spring temperatures, cooler summers and warmer falls relative to adjacent areas. During the period 1987–2017, the average annual high temperature at Kalispell was 12.3°C (WRCC, 2017). Average annual precipitation in the val-

ley during the same period averaged 403.8 mm/year. Precipitation was higher during the 1990s and lower from 2000 to 2009 (Rose, 2018).

Land use in the study area includes irrigated and dryland agriculture as well as residential development. Irrigated agriculture has shifted over several decades from surface-water flood irrigation to sprinkler and pivot irrigation using groundwater (Kendy & Tresch, 1996). Residential development has increased steadily since 1990. Much of this new development has been in former agricultural land.

The purposes of this study are to (1) test the capabilities of gravity data in detecting the buried troughs already known to exist in some configuration under the Flathead Valley and (2) identify any possible extensions of these troughs.

GEOLOGICAL AND HYDROGEOLOGICAL SETTING

Previous work has detailed the geology and hydrogeology of the study area. The Flathead Valley is a structural depression in metasedimentary basement rocks of the Mesoproterozoic Belt Supergroup. The top of this basement dips steeply eastward (Smith, 2004b). Harrison et al. (1992), Smith et al. (2000) and Smith (2004a) mapped surficial geology in the study area and its environs. The valley is partially filled with locally derived fluvial, glacial and lacustrine sediments and sedimentary rocks (Figure 1) ranging in age from late Eocene to Holocene (Smith, 2004b, 2004c, 2004d, 2004f). Unconsolidated Pleistocene alluvial sand and gravel host the deep alluvial aquifer in the valley as shown in the schematic cross section in Figure 2. Atop these alluvial sediments lies an interval of glacial till and lacustrine deposits forming a thick confining unit (Figure 2). This confining unit forms a hydraulic barrier between the deep aquifer below and Holocene terrace sands and gravels, deltaic deposits and the alluvium of modern streams, all of which overlie the lacustrine–till confining unit (Smith, 2004a, 2004e). Multiple shallow aquifers are hosted by the alluvium of modern streams in the Flathead Valley (Figure 2). Rose (2018) created a detailed three-dimensional hydrostratigraphic model of the Flathead Valley using hundreds of well logs, geological maps and gravity and seismic data.

The hydrostratigraphic units of the Flathead Valley have been classified in ascending stratigraphic order described below.

Bedrock aquifer

The Belt Supergroup forms the sides and the floor of the half graben underlying the Flathead Valley (Figures 2 and 3 a, b). These rocks are highly fractured and, where those fractures are connected, they confer a significant amount of secondary porosity. Such fractures transmit water from outcropping formations to deeper groundwater flow systems under the valley. Water wells are drilled into fracture systems along the margins of the Flathead Valley and in other places where the Belt Supergroup lies at shallow depths. The bedrock aquifer is characterized by transmissivity from 2.69 to 1252.33 m^2/d; with a geometric mean of 58.34 m^2/d and a storativity from 9×10^{-5} to 8.7×10^{-3} p (Rose et al., 2022).

Tertiary sediments

Tertiary sediments (Figures 3 a,b) form a deep confined aquifer lying atop the Belt Supergroup rocks under the valley (LaFave et al., 2004), but much additional work – well outside the scope of this paper – will be required to verify the age of such strata. Recent drilling intercepted lithologically distinct strata interpreted to be Tertiary in age at a depth of 366 m (Montana Groundwater Information Center [GWIC] ID 317,644; Bobst et al., 2022). On the basis of gravimetric and seismic data, the depth of these sediments ranges from 457 to 914 m (Smith, et al., 2000; Konizeski et al., 1968, Gibson, 2012).

Deep alluvial aquifer

The deep alluvial aquifer (Figure 3 a,b) is hosted by Quaternary alluvial sand and gravel that have local clay – and silt-rich zones near the top of the stratigraphic interval (Rose, 2018). Smith et al. (2000) interpreted these sediments to be alluvium, including outwash deposits.

According to Rose (2018), the top of the deep alluvial aquifer lies at depths of about 30.5–241 m. The upper contact of the unit undulates, but it dips overall to the south at 3.6 m/km or 19 feet per mile (Figures 1 and 3b). The maximum drilled penetration of this unit is 244 m (Bobst, 2022, personal communication). Estimates of total unit thickness in well logs range from >111 m (Konizeski et al., 1968) to as much as 305 m (Alden, 1953).

The well-sorted and coarse-grained unconsolidated sediment of the deep alluvial aquifer has inherently high porosity and permeability (Smith, 2004b). Moreover, it has a comparatively great saturated thickness, making it particularly productive. The number of wells and the cumulative annual volume of groundwater rights from the deep alluvial aquifer increased sharply in the mid-1970s in the study area. Nearly 60% of all groundwater rights in the study pertain to the deep alluvial aquifer (Montana State Library, 2022). The deep alluvial aquifer is a confined aquifer except in areas with no confining materials. The transmissivity of this aquifer ranges from 3.34 to 9120.47 m^2/d with a geometric mean of 429.39 m^2/d. The storativity ranges from 10^{-6} to 0.39 (Rose et al., 2022).

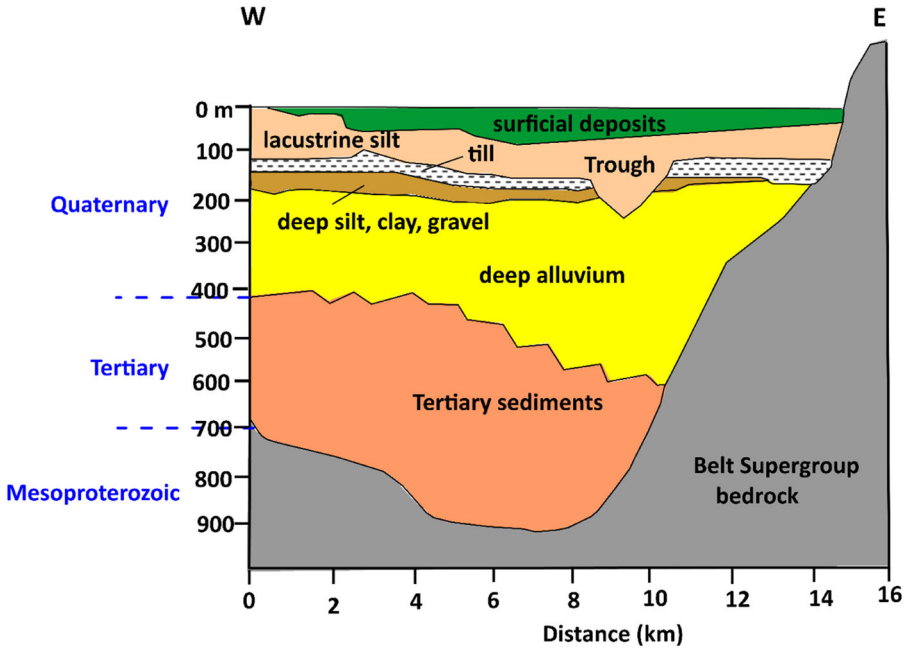

Figure 2 Generalized W-E schematic cross section of the Flathead Valley, sediments and sedimentary rocks ranging in age from upper Eocene to Holocene fill the half-graben produced by faulting in the metasedimentary rocks of the Belt Supergroup. Quaternary sediments (surficial deposits, lacustrine silt, till, deep sand and gravel, and deep alluvium) comprise more than half of the valley filled in depth. A sediment-filled trough is eroded through till and immediately underlying sediments, and it penetrates the deep alluvium, which hosts the deep alluvial aquifer (from Rose, 2018; reproduced with permission from the Montana Bureau of Mines and Geology).

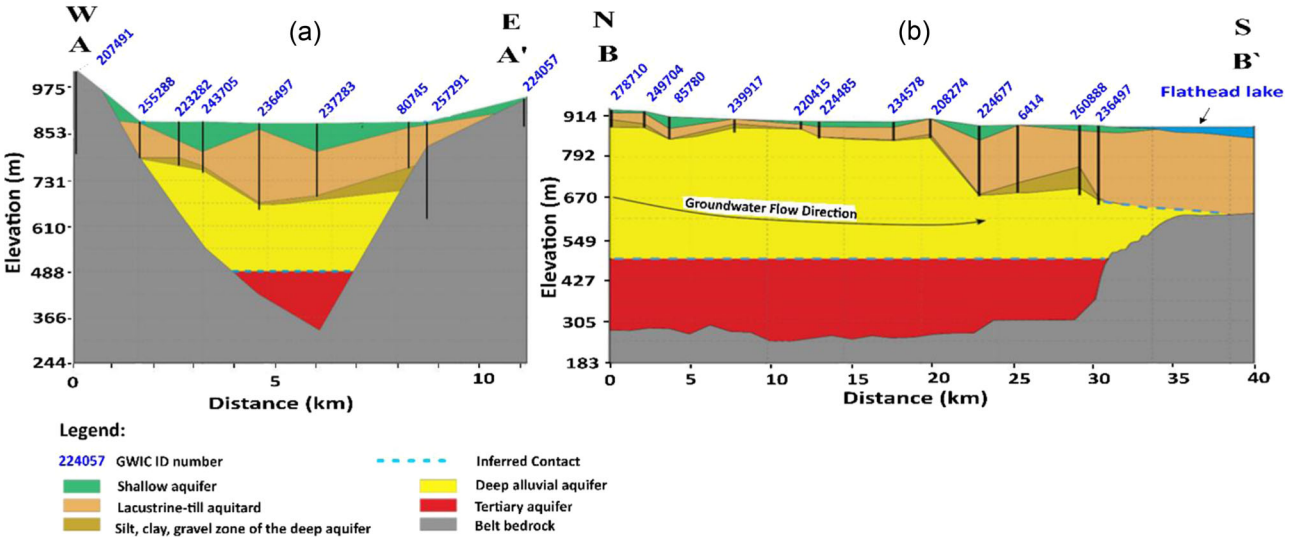

Figure 3 (a) Cross-section A–A′(Figure 1) is the hydrostratigraphy of the Flathead Valley, showing Belt Supergroup bedrock, Tertiary aquifer, Deep alluvial aquifer, gravel zone of the deep alluvial aquifer, lacustrine–till aquitard and shallow aquifer. Black vertical lines represent wells identified by their GWIC ID number, (b) Cross-section B–B′ (Figure 1) shows the deep alluvial aquifer in the Flathead Valley, which probably thins towards the north shore of Flathead Lake as the confining unit thickens (from Rose, 2018; reproduced with permission from the Montana Bureau of Mines and Geology).

Lacustrine–till aquitard

This hydrostratigraphic unit includes both till and lacustrine sediments averaging about 61 m in thickness and attaining a maximum thickness of 241 m (Konizesk et al., 1968; Hofmann & Hendrix, 2010; Rose, 2018). After the deglaciation of the Flathead Lobe of the Cordilleran Ice Sheet, a proglacial lake, the direct precursor of the present Flathead Lake, filled most of the valley (Smith, 2004a; Hofmann & Hendrix, 2010). Thick and

probably continuous fine-grained lacustrine sediments accumulated directly over the till. Where these sediments have not been identified in well logs, they may have been removed by erosion (Smith, 2004a). However, even though the lacustrine sediments may be only a few metres in thickness locally, it is impossible to confirm that the unit is absent at any location (Rose, 2018). The lacustrine–till aquitard is probably a continuous, valley-wide hydrostratigraphic unit (Rose, 2018).

The lacustrine–till aquitard limits the downward seepage of recharge from the valley floor and shallow aquifers to the deep alluvial aquifer. It also limits deep groundwater discharge to surface water where upward gradients exist. Nevertheless, groundwater moves slowly through this aquitard. The transmissivity and hydraulic conductivity are estimated from a single aquifer test to be approximately 0.018 m^2/d and 0.00021336 m/d, respectively (Rose et al., 2022).

Troughs

Several north-south trending deep troughs were eroded through the lacustrine–till aquitard and into the deep alluvial aquifer during the Quaternary and subsequently filled with sediments (Smith, 2004g; Rose, 2018). Figure 4 shows the location of wells and the troughs identified by the borehole data. Some of the troughs attain 1.6 km in width and 6 km in length (Figures 2 and 4). Lacustrine silts and clays, which were deposited in the proglacial precursor of present Flathead Lake, overlie the deep alluvial sediments and are the major component of trough-filling sediments. The deep portions of the troughs may contain some alluvial silt, sand and gravel, but because they are filled chiefly by fine-grained sediment, we include the trough-filling sediments in the lacustrine–till aquitard. Thus, the filled troughs are likely to have lower hydraulic conductivities than both the lacustrine–till aquitard and the shallow aquifer, and they should act as barriers that retard the lateral movement of groundwater flowing from more conductive zones. This scenario probably applies to the eastern side of the study area near the Swan Range (Figure 2).

Shallow aquifers

The shallow aquifers are hosted by surficial sediments lying above the lacustrine–till aquitard. The alluvium of modern streams and deltaic sediments is the dominant component (Smith,et al., 2000; Rose, 2018). The total thickness of the surficial deposits is less than 61 m (Rose, 2018; Figures 2 and 3a). North of Kalispell, the alluvium of extant streams ranges, several metres to as much as 15 m in thickness. The transmissivity ranges from 10.76 to 16,183.71 m^2/d; with a geometric mean of 294.87 m^2/d. The storativity, calculated from a single aquifer test, is 0.9 (Rose et al., 2022).

GRAVITY DATA ANALYSIS

Bouguer gravity map

The Bouguer gravity map of the study area (Figure 5 a,b) shows gravity variations resulting from lateral changes in density in the subsurface. Data for this map are legacy data collected nearly six decades ago by the Montana Bureau of Mines and Geology (Konizeski et al., 1968) and referred to the Kalispell airport station which has a value of 980.5819 Gal (Woollard, 1958). The grid of the gravity data (Figure 5a) consists of 497 data points on an approximate 1-mile (1.609 km) station distance. The data were collected by the portable compact temperature-compensated Worden gravity meter with a precision of 0.05 mGal and originally subjected to drift, latitude, free air, Bouguer and terrain corrections.

There is a large and elongated gravity low in the eastern part of the Flathead Valley (blue and purple tones in Figure 5a,b), in the vicinity of the Swan River and parallel to the Swan Range. It consists of distinct northern and southern parts. The northern part is located around the Flathead River between Creston and Columbia Falls, Montana (Figure 5b). The southern part of this elongated gravity low curves southeastward in the vicinity of Echo Lake (Figure 5b). There is also an elongated gravity high on the western side of the valley (orange to red tones), extending northwest-southeast from Rhodes to Somers, Montana. It is worth noting that the gravity anomalies matched well with the known geology of the valley. An elongated gravity low in the eastern part of the valley is associated with the existence of low-density Cenozoic deposits in the valley, whereas the elongated gravity high in the western part of the valley exists where there are exposures of the belt supergroup bedrock at the periphery of the valley.

Different filters and techniques, based on derivative calculations, can be used in space and frequency domains to identify abrupt density changes and to enhance linear features in gravity map. We calculated the first and the second directional derivatives in the space domain. We conducted two-dimensional (2D) Fourier transform analyses by using the fast Fourier transform (FFT) algorithm (Claerbout, 1976; Pirttijarvi, 2014). After we calculated the FFT, we implemented frequency filtering (Pirttijarvi, 2014). We computed six edge detection techniques: (1) horizontal gradient *H*; (2) total gradient *A* (analytic signal); (3) maximum horizontal gradient (MHG; total horizontal derivative); (4) theta map (TM); (5) tilt gradient (TG) *T;* and (6) generalized derivative (GD).

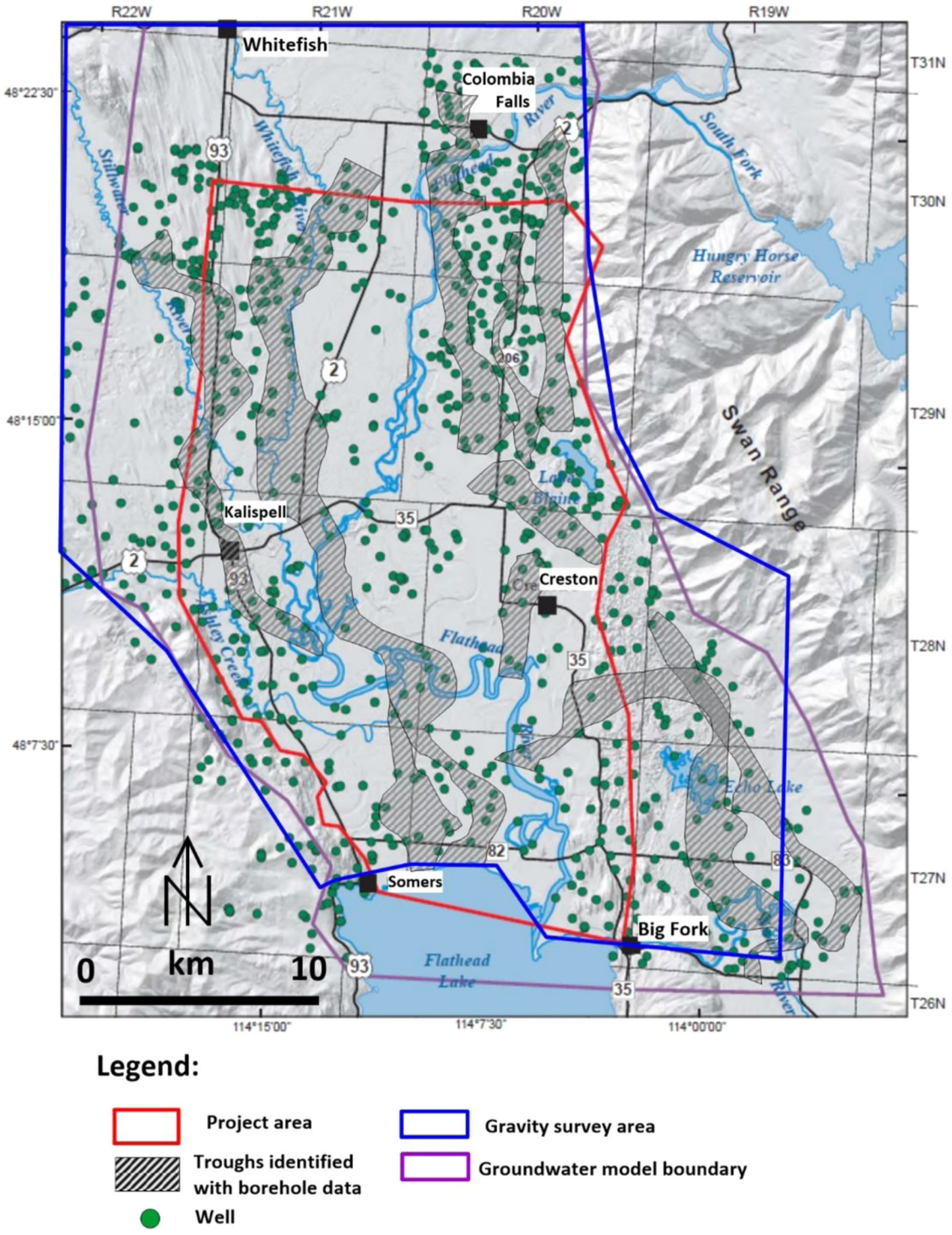

Figure 4 Flathead Valley study area –showing the gravity survey area – has numerous north-south trending deep troughs eroded through lacustrine sediments and till and into the top of the deep alluvial aquifer. Green dots represent the location of wells (from Rose, 2018; reproduced with permission from the Montana Bureau of Mines and Geology).

Directional derivatives

Directional derivatives provide information about the rate of change of the slope computed from the Bouguer gravity data in a specified direction. Using directional derivatives enables us to select the best direction (angle) that shows the abrupt change in the gravity data, and hence to locate the boundaries between geological bodies with different densities. We calculated the directional derivatives in the space domain. However,

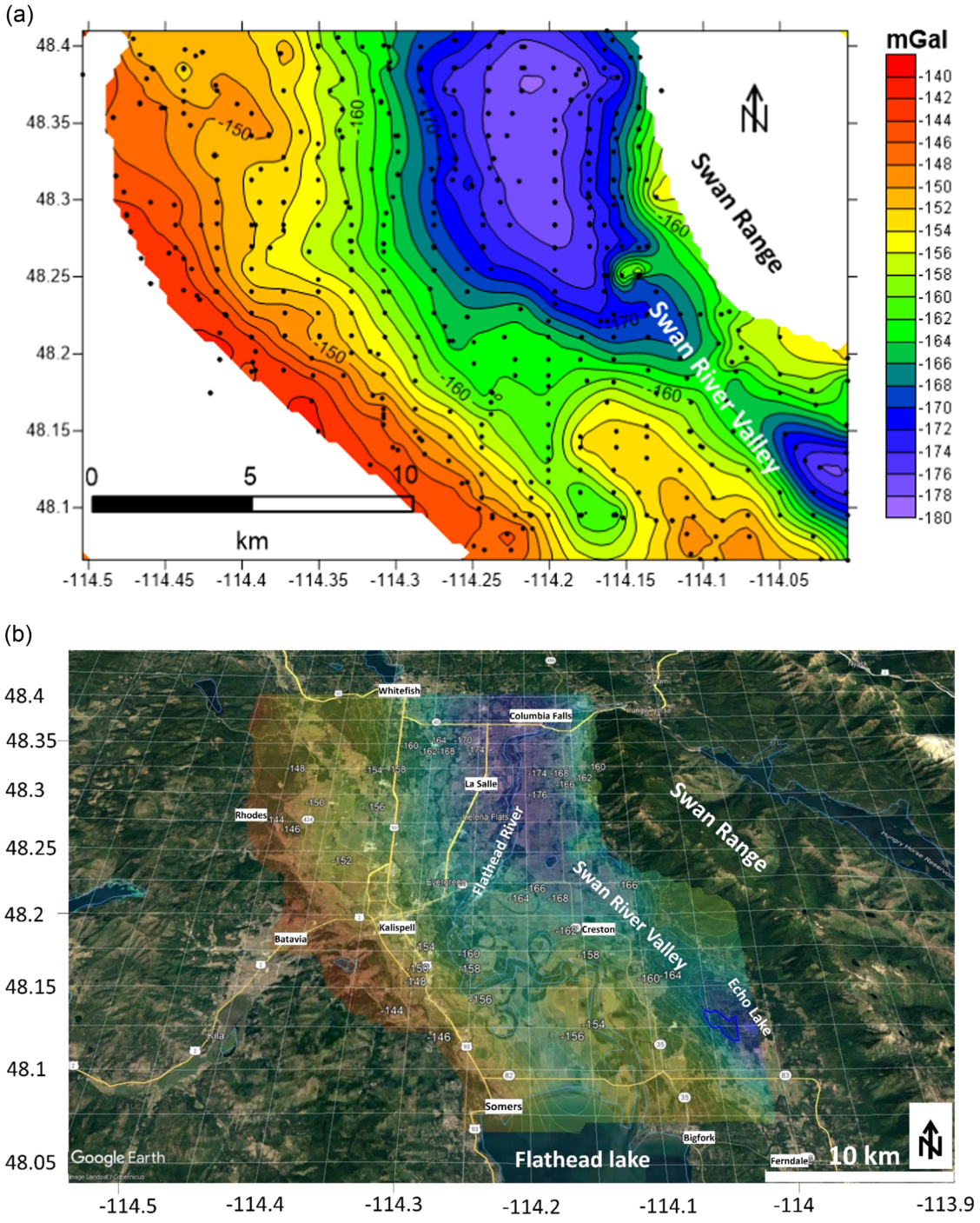

Figure 5 Bouguer gravity map of the Flathead Valley generated from legacy gravity data after Konizeski et al. (1968). Dots represent the location of gravity data (a). Gravity values superimposed on a base photograph of the study area from Google Earth dated May 2023 (b) to match with the geology of the valley.

computation in the space domain is still preferred in certain conditions and applications, especially to smooth noisy signals (Demarco et al., 2023). From the Bouguer gravity map of the study area (Figure 5 a,b), We calculated the first horizontal directional derivative (FHD), the second horizontal directional derivative (SHD), and matched between the results of both.

First horizontal directional derivative map

FHD or directional derivative (Figure 6a) calculates the slope of the surface along a given direction defined by the angle (α). FHD of a map dataset (f) is calculated by the Schwartz equation (1974), where the directional derivative ($\frac{df}{ds}$) at a point is equal to the dot product

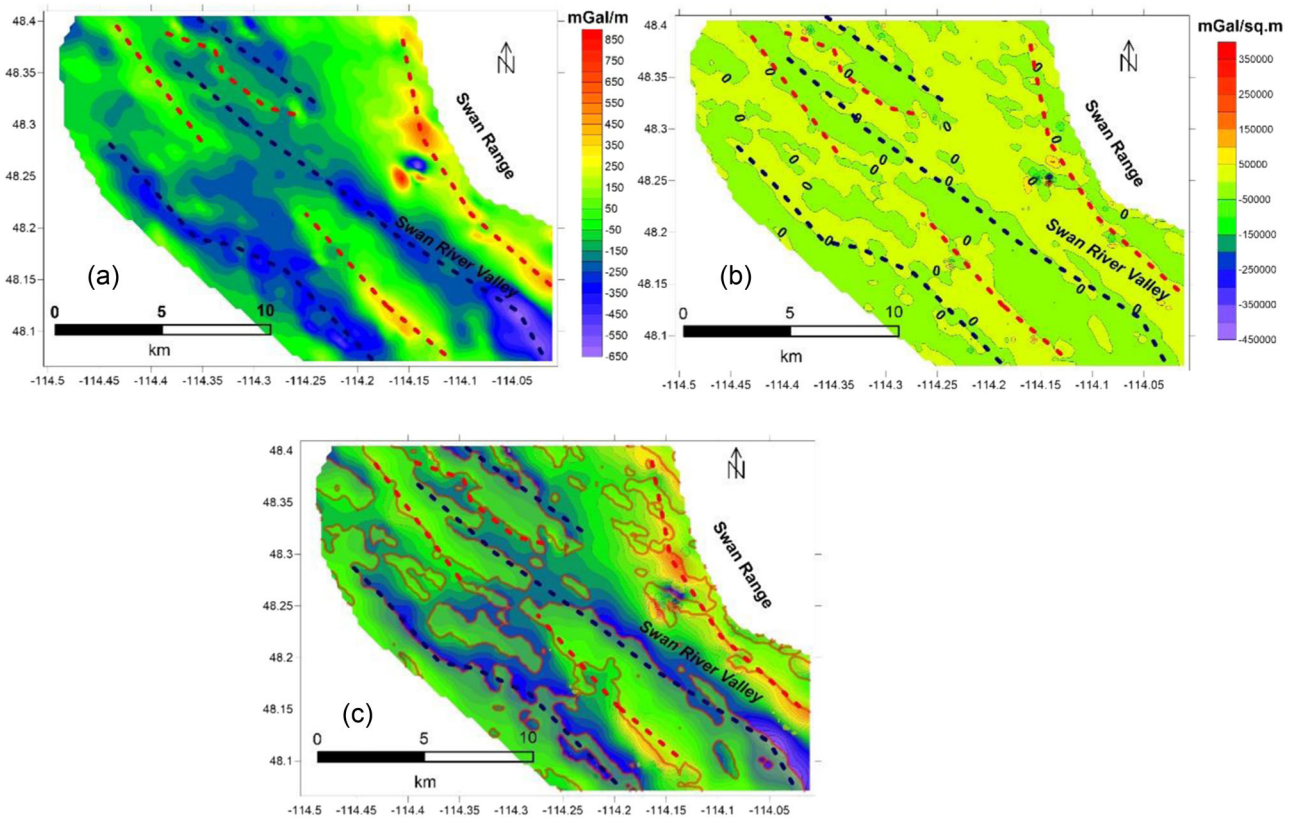

Figure 6 (a) First horizontal directional derivative at E45°N; the red dashed lines and blue dashed lines on the map outline the maximum and minimum values, respectively. (b) The second horizontal directional derivative at E45°N. (c) Superposition of the first horizontal derivative on the second directional derivative at E45°N; note the very close correspondence of the trough edges outlined by the two derivatives. (See the text for additional discussion.)

between the gradient vector ($\vec{g}$) and a unit vector in the direction of interest (α):

$$\frac{df}{ds} = \vec{g}.\begin{bmatrix}\cos(\alpha)\\ \sin(\alpha)\end{bmatrix} = \left[\frac{df}{dx}, \frac{df}{dy}\right] . \begin{bmatrix}\cos(\alpha)\\ \sin(\alpha)\end{bmatrix}, \quad (1)$$

$$\frac{\partial f}{\partial s} = \frac{\partial f}{\partial x}.\cos(\alpha) + \frac{\partial f}{\partial y}.\sin(\alpha), \quad (2)$$

where $\alpha = \pm \pi/2$ radians, $\partial f/dx$ and $\partial f/dy$ are the horizontal derivatives in x and y directions, respectively. The α angle is chosen as E 45° N, which is approximately perpendicular to the assigned troughs from borehole data (Figure 4). FHD can identify vertical contact between sub-surface rocks and enhance edges and other linear features in the data. The maximum (positive) and minimum (negative) values of FHD can reveal faults or abrupt lithological changes. The positive or negative value of the first derivative depends on the slope direction. If the slope of the gravity data is uphill, the derivative is positive; and if the slope is downhill, the derivative is negative (Schwartz, 1974; Tuma, 1979). The red and blue dashed lines on the map (Figure 6a) outline the maximum and minimum values of FHD, respectively.

Second horizontal directional derivative map

The second derivative calculates the rate of change of slope (FHD) along a given direction, which therefore is like the curvature of the gravity field. It represents the directional derivative of the first directional derivative (Schwartz, 1974), as shown in Equation (3):

$$\frac{\partial^2 f}{\partial s^2} = \frac{\partial^2 f}{\partial x^2}.\cos^2(\alpha) + 2\frac{\partial^2 f}{\partial x\,\partial y}.\cos(\alpha).\sin(\alpha) + \frac{\partial^2 f}{\partial y^2}.\sin(\alpha). \quad (3)$$

A second derivative map (Figure 6b) is useful for identifying the positions of small, shallow anomalies and suppressing regional anomalies (Burger, 1992), which suits our case study.

Matching between the first and the second derivative map (Figure 6c) shows that the second derivative shallow anomalies, which extend in the northwest to southeast directions, are outlined by the maximum (positive) and minimum (negative) values of the first

derivative (red and blue dashed lines) to the east and west, respectively.

Edge detection techniques

Our edge detection techniques use gradients derived from gravity data. Such derived gradients enhance small, low-amplitude features, thereby locating and delineating geological anomalies. In the present study, we apply six types of filters in edge detection: (1) horizontal gradient *H*; (2) total gradient *A* (analytic signal); (3) *MHG* (total horizontal derivative); (4) TM; (5) TG *T;* and (6) GD.

Total horizontal gradient (*H*)

A tabular body of geological material, such as a layer of rock or sediment, should produce a gravity anomaly with steep gradients corresponding to the edges of the body. If an edge is vertical and well-separated from other features, then the steepest anomaly should be directly over the edge (Blakely, 1995). The horizontal gradient is easily calculated using a simple finite-difference relationship:

$$H = \sqrt{\left(\frac{\partial f}{\partial x}\right)^2 + \left(\frac{\partial f}{\partial y}\right)^2}, \tag{4}$$

where $\partial f/\partial x$ and $\partial f/\partial y$ are the horizontal derivatives in the *x* and *y* directions, respectively.

Total gradient *A* (analytic signal)

The total gradient or *analytic signal* is formed through a combination of the horizontal and vertical gradients (Salem & Ravat, 2003; Salem, 2005; Demarco et al., 2023). It enhances the edges of features in all azimuths. The amplitude of the analytic signal ($|As|$) is given by:

$$|As| = \sqrt{\left(\frac{\partial f}{\partial x}\right)^2 + \left(\frac{\partial f}{\partial y}\right)^2 + \left(\frac{\partial f}{\partial z}\right)^2}, \tag{5}$$

where $\partial f/\partial x$ and $\partial f/\partial y$ are the horizontal derivatives in the *x* and *y* directions, respectively, and $\partial f/\partial z$ is the vertical derivative.

Maximum horizontal gradient

The MHG can be used to locate the boundaries between geological bodies with different densities (Blakely & Simpson, 1986). It is a very robust method for picking the reliable maximums on a transformed map. This method involves the calculation of a horizontal gradient and comparison of the horizontal gradient of a centre point with its eight nearest neighbours in four directions within each 3×3 calculation grid. The horizontal location and magnitude of the maximum values are found by interpolating a second-order polynomial through the trio of points provided that the magnitude of the middle point is greater than its two nearest neighbours in one direction (Van Kha et al., 2018).

Theta map

TM is an edge-detecting filter that divides the total horizontal derivative in the numerator by the analytic signal amplitude (total gradient) in the denominator as shown in Equation (6) (Wijns et al., 2005):

$$\theta = \cos^{-1}\left(\frac{\left(\left(\frac{\partial f}{\partial x}\right)^2 + \left(\frac{\partial f}{\partial y}\right)^2\right)^{1/2}}{|As|}\right), \tag{6}$$

where:

$$|As| = \sqrt{\left(\frac{\partial f}{\partial x}\right)^2 + \left(\frac{\partial f}{\partial y}\right)^2 + \left(\frac{\partial f}{\partial z}\right)^2}.$$

This filter enhances the edges of features of all azimuths.

Tilt gradient

The TG or tilt angle is defined as the arctan value of the ratio of the vertical derivative of the potential field to its horizontal derivative (Miller & Singh, 1994; Verduzco et al., 2004). The TG is a balanced derivative and has both vertical, horizontal and hyperbolic forms (Miller & Singh, 1994, Cooper & Cowan, 2006).

Because the TG is an arctan trigonometric function, the tilt amplitudes are restricted to values between −90° and +90° and the boundaries of the source body are defined by means of the tilt angle. The contours of a positive tilt angle define the source body itself, and the contours of a negative tilt angle represent the outside of the source body. The zero contour represents the vertical boundary of the source body (Miller & Singh, 1994). The TG method is potentially less sensitive to noise compared to higher order derivatives' methods (Akin et al., 2011).

$$T = \tan^{-1}\left(\frac{\frac{\partial f}{\partial z}}{\sqrt{\left(\frac{\partial f}{\partial x}\right)^2 + \left(\frac{\partial f}{\partial y}\right)^2}}\right). \tag{7}$$

Generalized derivative

The GD map is the most efficient technique for calculating different types of derivatives from large datasets. The GD is a linear combination of the horizontal and vertical field derivatives, normalized by the analytic signal amplitude (Cooper & Cowan, 2011).

The GD can be used to enhance small and linear features in the data. This is accomplished by altering the direction of illumination (or gradient direction) defined by two angles, elevation from the vertical axis and azimuth from the positive *x*-axis (Cooper & Cowan, 2011).

The generalized derivative operator (GDO) can be produced by dividing the field derivative in three dimensions (*x*, *y*, *z*) in the numerator by the analytic signal amplitude (total gradient) in the denominator as shown in Equation (8) (Cooper & Cowan, 2011).

$$\mathrm{GDO} = \frac{\left(\frac{\partial f}{\partial x}\sin\theta + \frac{\partial f}{\partial y}\cos\theta\right)\cos\emptyset + \frac{\partial f}{\partial z}\sin\emptyset}{|As|}, \quad (8)$$

where:

$$|As| = \sqrt{\left(\frac{\partial f}{\partial x}\right)^2 + \left(\frac{\partial f}{\partial y}\right)^2 + \left(\frac{\partial f}{\partial z}\right)^2},$$

where θ is the azimuth in the horizontal plane and $\varnothing$ is the elevation in the vertical plane.

The GD allows the derivative of the field in any direction in three-dimensional space to be used.

We applied these filters to the gravity data from Flathead Valley to outline the edges of the buried troughs. From the 2D FFT, we calculated the same types of filters (1) horizontal gradient *H*, (2) total gradient *A* (analytic signal), (3) MHG (total horizontal derivative), (4) TM, (5) TG T and (6) GD. The GD map (Figure 7f) and the TG map (Figure 7e) outlined the same northwest-southeast-extending features, whereas the MHG (Figure 7c) outlined the same features with the maximum values of the gradient. The TM (Figure 7d) outlined the edges over the contact between the highest and lowest angles. The total gradient map (Figure 7b) shows blurry features with many anomalous closures distributed all over the area, whereas the MHG map (Figure 7c) located the edges over the steepest gradient.

DISCUSSION

Our analysis of legacy land-based gravity data from the Flathead Valley in northwestern Montana readily detected the edges and extensions of the erosional troughs filled with and buried by Quaternary sediments. This analysis applied directional horizontal derivatives and six types of edge detection techniques, namely (1) horizontal gradient *H*, (2) total gradient *A* (analytic signal), (3) MHG (total horizontal derivative), (4) TM, (5) TG *T* and (6) GD.

Figure 8 illustrates our results through the superposition of the GD contour map (Figure 7f) and the well-known locations of the troughs as determined from drilling (Figure 4). We used the GD map because this filter responds to the whole source (i.e., the anomalous body) as well as its edges. The sediment-filled troughs determined by mapping borehole data alone are marked by numbers 1–10 in Figure 8, and the sharp yellow contours on the GD map (Figure 7f) approximate the zero-contour line that separates different rock densities and indicates abrupt lithological changes. Close examination of the map shows that: (1) all troughs (numbers 1−10) fit between the yellow contours; (2) the GD map shows that troughs numbers 1, 2, 3 and 8 have northern extensions in area A and might be connected in area C; (3) trough number 4 is connected with troughs 6 and 7 in area B to the south, and it is also connected with trough number 3 to the north; (4) areas D, E, F and G exhibit inferred troughs where there are few boreholes at these areas (Figure 4); and (5) small dissected zones a, b, c, d and e in the northwestern zone of the survey area might represent an inferred dissected trough. The same results could also be observed on the TG contour map (Figure 9).

Some of the calculated directional derivatives, such as the first horizontal derivative and the second horizontal derivative (Figure 6 a,b), indicated the approximate extent of the sediment-filled troughs under the Flathead Valley, but they failed to outline their exact locations because these derivates are directional derivatives. Directional derivatives calculate the slope of the surface along a given direction (E45°N), which is approximately perpendicular to the assigned troughs from drilled wells and cannot calculate derivates in two or three dimensions (*x*, *y*, *z*). The GD map (Figure 7f) is more efficient in outlining the troughs because it is a linear combination of the horizontal and vertical field derivatives, normalized by the analytic signal amplitude. The TG or tilt angle (Figure 7e) is also efficient because of the different vertical, horizontal and hyperbolic types of derivatives calculated by these methods.

Basin-fill or valley-fill aquifers, like those under the Flathead Valley in Montana, are very important local to regional sources of groundwater in many parts of the USA, Canada and elsewhere (Ehlers &Linke, 1989; Allen & Milenic, 2003; Kappel & Miller, 2005; Dragon, 2006; Cummings et al., 2012; Kerr et al., 2015; Kotowski & Kachnic, 2016; Sharpe et al., 2018). These kinds of aquifers are hosted by sediments deposited within elongate depressions produced by tectonics and/or erosion by streams or glaciers. Moreover, they typically exhibit complexities in their sedimentary architecture

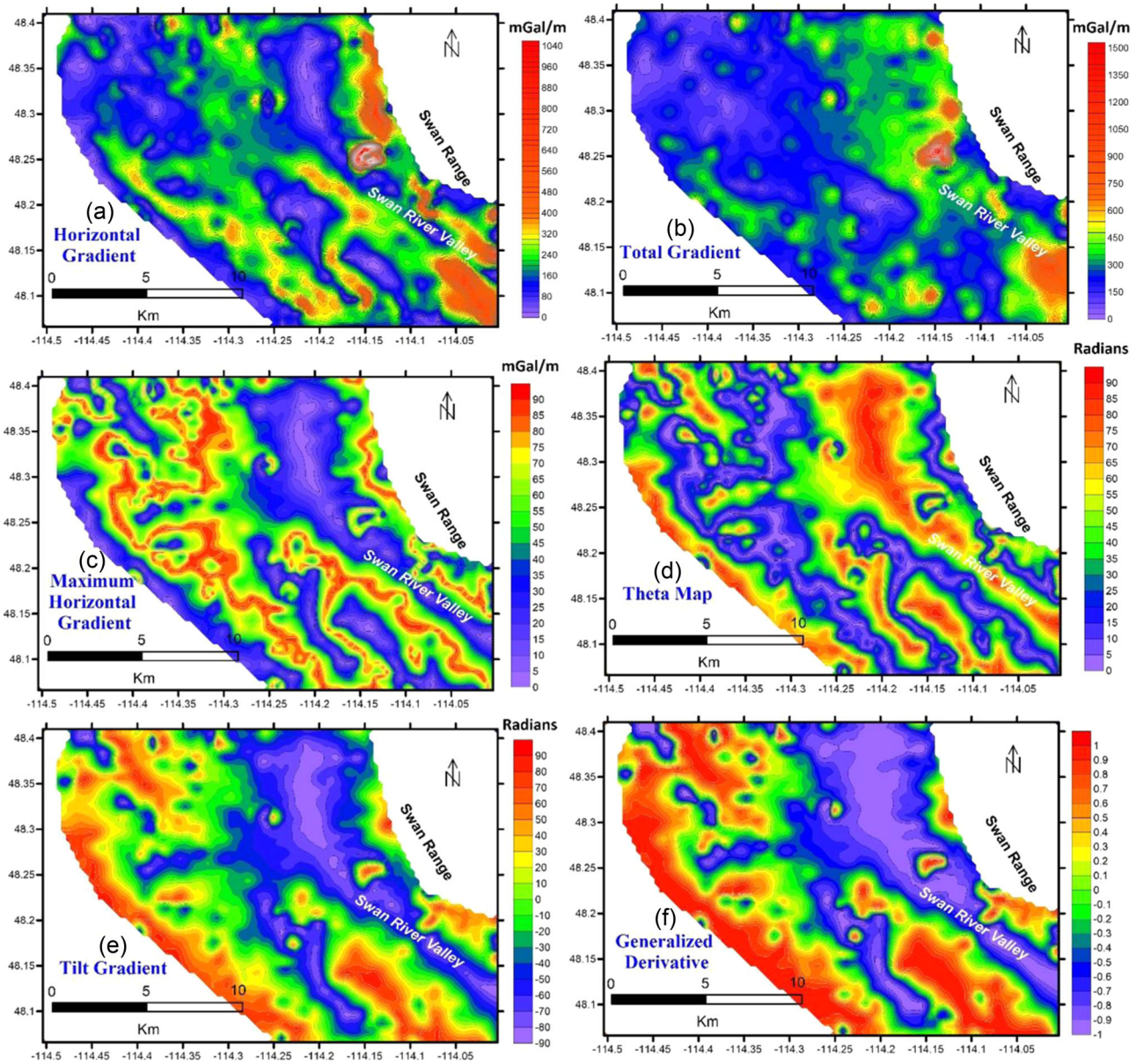

Figure 7 (a) Horizontal gradient map, (b) total gradient, *A* (analytic signal) map, (c) maximum horizontal gradient map, (d) theta map, (e) tilt gradient map, (f) generalized derivative map (elevation 45°, azimuth 45°).

and hydrostratigraphy as well as in their relationships with the bedrock that confines them and with any adjacent aquifers. Basin- or valley-fill aquifers are particularly important in the western one-third of the contiguous USA, including the present study area (Planert & Williams, 1995; Robson & Banta, 1995;; Houston et al., 2015). Geophysical methods, especially electromagnetic (EM) surveys, have greatly enhanced the understanding of some basin- or valley-fill aquifers in North America and Europe (e.g., Gabriel et al., 2003; Huuse et al., 2003; Pugin et al., 2014, Høyer et al., 2015; Korus et al., 2017). However, airborne electromagnetic (AEM) surveys require a significant capital investment and ground-based EM surveys require major commitments in personnel time. (e.g., Steuer et al., 2009). Both types of surveys require relatively sophisticated equipment. These restrictions could preclude the application of more sophisticated geophysical surveys at certain times and in many places. As we have demonstrated, legacy gravity data can be an important – and likely cost-free – resource for a rapid assessment of at least some aspects of valley- or basin-fill geology as they pertain to groundwater. Thus, an analysis such as ours could either (1) economically augment an existing study based on borehole data or (2) provide additional impetus for attaining the funds or equipment to perform comprehensive AEM surveys in a critical area.

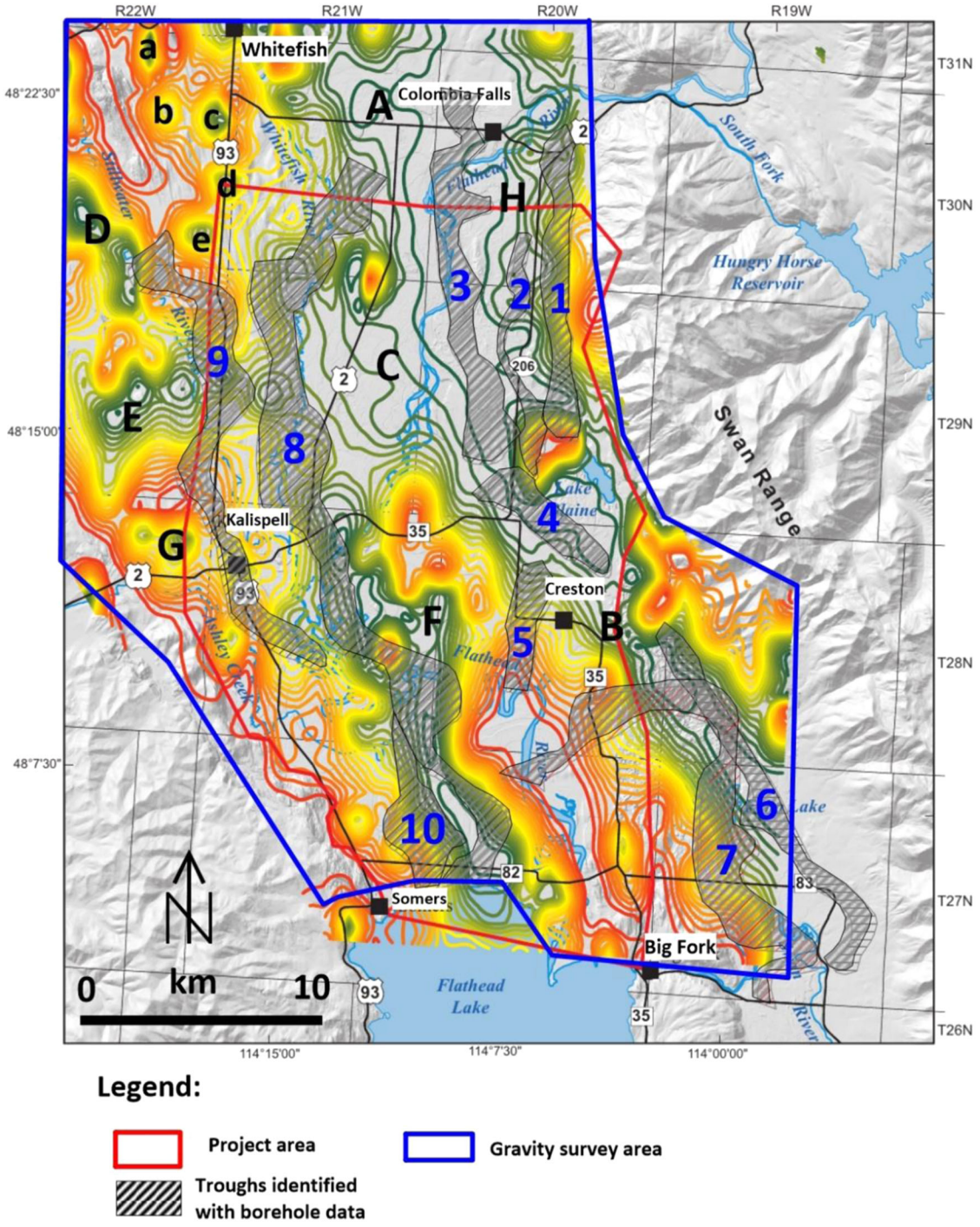

Figure 8 A Generalized derivative contour map superimposed on the locations of erosional troughs determined previously from borehole data (cross-hatched and numbered 1–10). Letters A, B, C, D, E, F, G, a, b, c, d are inferred parts of the troughs that were not identified by drilling.

CONCLUSIONS

We conclude that borehole data, although eminently important in understanding local hydrostratigraphy, were insufficient in density to fully delineate buried, sediment-filled troughs that play important roles in the hydrogeology of the Flathead Valley in Montana. Different edge-detection techniques – applied in both space and frequency domains to a Bouguer gravity map that we generated from legacy (1968) gravity data – greatly enhanced the spatial resolution of the troughs. The GD, MHG, total gradient and TG that we calculated from the Bouguer gravity map were especially useful in hitherto unrecognized parts of the troughs. Moreover, a

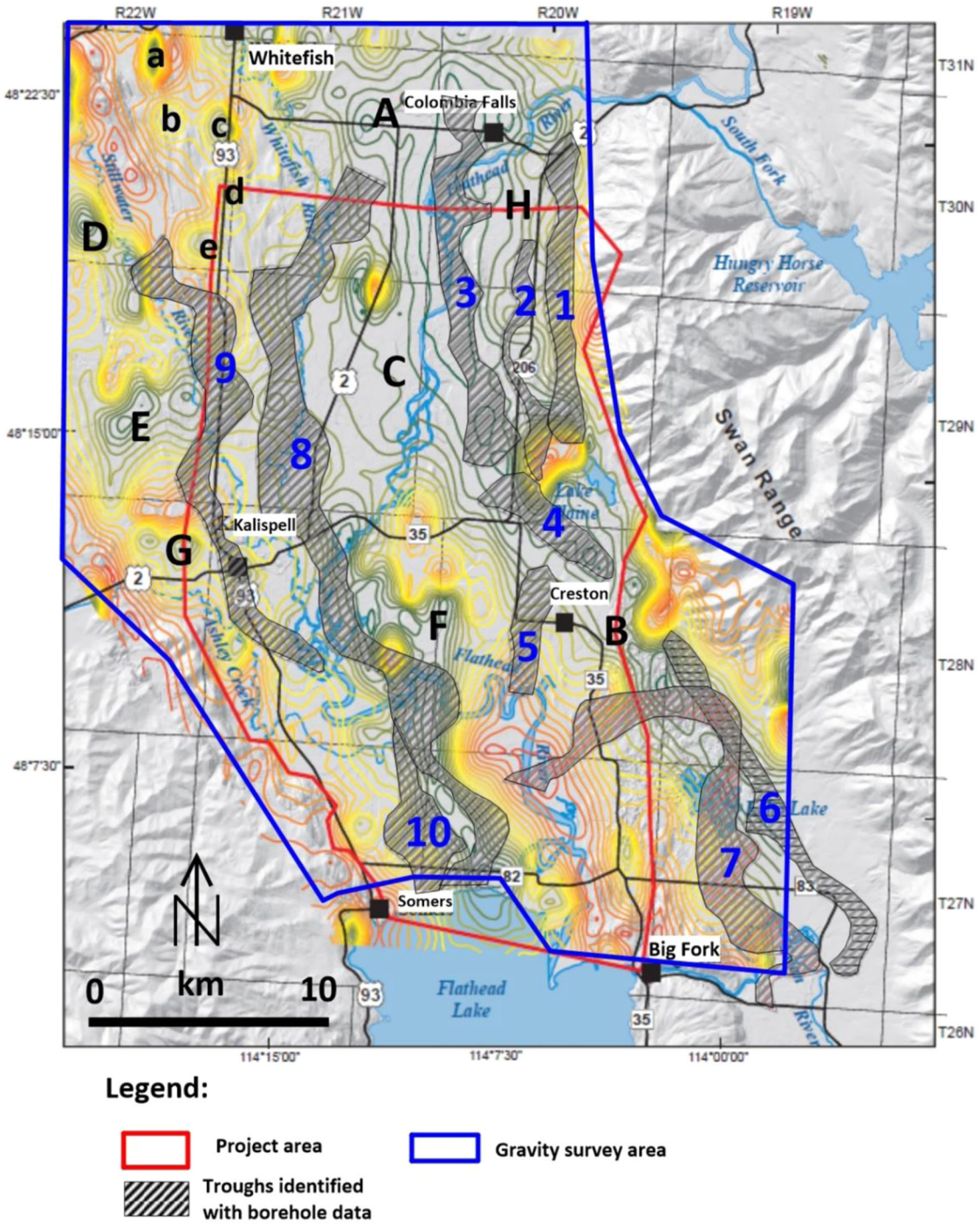

Figure 9 Tilt gradient contour map superimposed on the locations of erosional troughs determined previously from borehole data (cross-hatched and numbered 1–10). Letters A, B, C, D, E, F, G, a, b, c, d are inferred parts of the troughs that were not identified by drilling.

careful comparison between our calculated derivatives and existing borehole data allowed us to infer that extensions of the buried troughs exist in the northern and northwestern parts of the study area. These extensions roughly coincide with the courses of the Stillwater, Whitefish and Flathead rivers. Furthermore, our analysis suggests that some of the buried troughs in the southeastern part of the surveyed area around the Swan River are laterally connected, and this is a new and important result that changes the perspective on overall groundwater flow in the study area. Future work in the Flathead Valley should seek to determine the depths and exact widths of the buried troughs as well as the saturated thicknesses and groundwater flow directions in the sediments that fill them. Such investigations could be accomplished by integrating the methods we have

described herein with other geophysical techniques, particularly electrical resistivity tomography, time domain electromagnetic and self-potential surveys. Our success portends that the reanalysis and reinterpretation of legacy gravity data in settings broadly similar to the Flathead Valley may greatly improve the understanding of local and regional hydrostratigraphy.

Funding Information

None

ACKNOWLEDGMENTS

The authors acknowledge the Montana Bureau of Mines and Geology, Butte, Montana, for providing the gravity data analysed in this paper and for giving access to all related geological and hydrogeological reports.

CONFLICT OF INTEREST STATEMENT

We declare that there are no conflicts of interest in this work.

DATA AVAILABILITY STATEMENT

The dataset analysed during the current study is available from the corresponding author on reasonable request or from the Montana Bureau of Mines and Geology, Butte, Montana, USA.

ORCID

Mohamed A. Khalil https://orcid.org/0000-0001-9514-7184

REFERENCES

Akin, U., Serifoglu, B., & Duru, M. (2011) The use of tilt angle in gravity and magnetic methods. *Bulletin of the Mineral Research and Exploration*, 143, 1–12. https://www.researchgate.net/publication/265467004.

Alden, W.C. (1953) Physiography and glacial geology of western Montana and adjacent areas (200 p.). United States Geological Survey Professional Paper 231.

Allen, A., & Milenic, D. (2003) Low-enthalpy geothermal energy resources from groundwater in fluvioglacial gravels of buried valleys. *Applied Energy*, 74, 9–19.

Amiri, A., Chaqui, A., Nasr, H., Inoubli, M.H., Ben Ayed, N., & Tlig, S. (2011) Role of preexisting faults in the geodynamic evolution of Northern Tunisia, insights from gravity data from the Medjerda valley. *Tectonophysics*, 506(1–4), 1–10. https://doi.org/10.1016/j.tecto.2011.03.004.

Barhoumi, A., Belkhiria, W., Ayari, J., Hatira, N., Braham, A., & Dhaha, F. (2021) Tectonic controls on the salt diapir-related Mississippi Valley-type lead-zinc mineralization of Fej El Adoum ore deposit (Northern Tunisian Atlas): constraints from detailed gravity and drill hole data. *Journal of African Earth Sciences*, 181, 104237. https://doi.org/10.1016/j.jafrearsci.2021.104237.

Blakely, R.J. (1995) *Potential theory in gravity and magnetic applications*. New York: Cambridge University Press.

Blakely, R.J., & Simpson, R.W. (1986) Approximating edges of source bodies from magnetic or gravity anomalies. *Geophysics*, 51, 1494–1498.

Bobst, A. (2022) Personal communication. Montana Bureau of Mines and Geology.

Bobst, A., Rose, J., & Berglund, J. (2022) An evaluation of the unconsolidated hydrogeologic units in the south-central Flathead Valley, Montana: Montana Bureau of Mines and Geology Open-File Report 752, 16 p.

Burger, H.P. (1992), *Exploration geophysics of the shallow subsurface*. Englewood, NJ: Prentice-Hall.

Claerbout, J. (1976) *Fundamentals of geophysical data processing. With applications to petroleum prospecting*. New York: McGraw-Hill.

Cooper, G.R.J., & Cowan, D.R. (2006) Enhancing potential field data using filters based on the local phase. *Computers & Geosciences*, 32, 1585–1591.

Cooper, G.R.J., & Cowan, D.R. (2011) A generalized derivative operator for potential field data. *Geophysical Prospecting*, 59, 188–194.

Constenius, K. (1996) Late Paleogene extensional collapse of the Cordilleran foreland fold and thrust belt. *Geological Society of America Bulletin*, 108, 20–39.

Cummings, D.I., Russell, H.A.J., & Sharpe, D.R. (2012) Buried Valley aquifers in the Canadian Prairies: geology, hydrogeology, and origin. *Canadian Journal of Earth Science*, 49, 987e.

Demarco, P., Bonilla, A., Bettucci, L., & Prezzi, C. (2023) Potential-field filters for gravity and magnetic interpretation: A review. *Surveys in Geophysics*, 44, 603–664. https://doi.org/10.1007/s10712-022-09752-x.

Dragon, K. (2006) Application of factor analysis to study contamination of a semi-confined aquifer (Wielkopolska Buried Valley aquifer, Poland). *Journal of Hydrology*, 331, 272–279.

Ehlers, J., & Linke, G. (1989) The origin of deep buried channels of Elsterian age in Northwest Germany. *Journal of Quaternary Science*, 4, 255–265.

Gabriel, G., Kirsch, R., Siemon, B., & Wiederhold, H. (2003) Geophysical investigation of buried Pleistocene subglacial valleys in Northern Germany. *Journal of Applied Geophysics*, 53, 159–180.

Gibson, R.I. (2012) Personal communication. Montana Bureau of Mines and Geology.

Harrison, J.E., Cressman, E.R., & Whipple, J.W. (1992) Geologic and structure maps of Kalispell 1 × 2-degree quadrangle, Montana and Alberta, British Columbia. United States Geological Survey: Miscellaneous Geologic Investigation I-2267, 1 sheet(s), 1:250,000.

Hofmann, M.H., & Hendrix, M.S. (2010) Depositional processes and the inferred history of ice-margin retreat associated with the deglaciation of the Cordilleran Ice Sheet: The sedimentary record from Flathead Lake, northwest Montana, USA. *Sedimentary Geology*, 223, 61–74.

Hofmann, M.H., Hendrix, M.S., Moore, J.N., & Sperazza, M. (2006) Late Pleistocene andHolocene depositional history of sediments in Flathead Lake, Montana: Evidencefrom high-resolution seismic reflection interpretation. *Sedimentary Geology*, 184, 111–131.

Houston, N.A., Thomas, J.V., Foster, L.K., Pedraza, D.E., & Welborn, T.L. (2015) Hydrogeologic framework and groundwater characterization in selected alluvial basins in the upper Rio Grande Basin, Colorado, New Mexico, and Texas, United States, and Chihuahua, Mexico, 1980 to 2015. United States Geological Survey Scientific Investigations Report 2021–5035, 71 p.

Høyer, A.-S., Jørgensen, F., Sandersen, P.B.E., Viezzoli, A., & Møler, I. (2015) 3D geological modelling of a complex buried-valley network delineated from borehole and AEM data. *Journal of Applied Geophysics*, 122, 94–103.

Huuse, M., Lykke-Andersen, H., & Piotrowski, J.A. (2003) Geophysical investigations of buried Quaternary valleys in the formerly glaciated NW European lowland: significance for groundwater exploration. *Journal of Applied Geophysics*, 53, 153–157.

Kappel, W.M., & Miller, T.S. (2005) Hydrogeology of the valley-fill aquifer in the Onondaga trough, Onondaga County, New York: U.S.

Geological Survey Scientific Investigations Report 2005–5007, 13 p.
Kendy, E., & Tresch, R.E. (1996) Geographic, geologic, and hydrologic summaries of intermontane basins of the Northern Rocky Mountains, Montana, U.S. Geological Survey, eBook, 233 p.
Kerr, P., Tassier-Surine, S., Streeter, M., & Gammon, J.M. (2015) Geologic evaluation of the buried sand and gravel aquifers of western Iowa. *Iowa Geological Survey Water Resources Investigation Report*, 14, 30.
Khalil, M.A., Santos, F M., & Farzamian, M. (2014) 3D gravity inversion and Euler deconvolution to delineate the hydro-tectonic regime in El-Arish area, northern Sinai Peninsula. *Journal of Applied Geophysics*, 103, 104–113. https://doi.org/10.1016/j.jappgeo.2014.01.012.
Khalil, M.A., Santos, F M., Farzamian, M., & Kenawy, A. (2015) 2-D Fourier transform analysis of the gravitational field of Northern Sinai Peninsula. *Journal of Applied Geophysics*, 2015.
Khalil, M.A., & Santos, F.M. (2015) Geophysical evidence for the hydrotectonic origin of the Sabkha El Sheikh Zwayed Lake and the shallow fresh water supplies, Northern Sinai, Egypt. *Near Surface Geophysics*, 13, 93–101. https://doi.org/10.3997/1873-0604.2014047<./bib>
Khalil, M.A., Santos, F.M., (2015b) Geophysical evidence for the hydrotectonic origin of the Sabkha El Sheikh Zwayed Lake and the shallow fresh water supplies, Northern Sinai, Egypt. *Near Surface Geophysics*, 13: 93–101. https://doi.org/10.3997/1873-0604.2014047
Konizeski, R.L., Brietkrietz, A., & McMurtrey, R.G. (1968) Geology and groundwater resources of the Kalispell Valley, northwestern Montana. *Montana Bureau of Mines and Geology: Bulletin*, 68, 42.
Korus, J.T., Joeckel, R.M., Divine, D.P., & Abraham, J.D. (2017) Three-dimensional architecture and hydrostratigraphy of cross-cutting buried valleys using airborne electromagnetics, glaciated Central Lowlands, Nebraska, USA. *Sedimentology*, 64: 553–581.
Kotowski, T., & Kachnic, M. (2016) The geochemical study of groundwaters from Cenozoic aquifers in the Gwda catchment (Western Pomerania, Poland). *Environmental Earth Sciences*, 75, 192.
LaFave, J.I. (2023) Montana Bureau of Mines and Geology, Personal communication.
LaFave, J.I. (2004) Potentiometric surface map of the southern part of the Flathead Lake area, Lake Missoula, Sanders Counties, Montana. Montana ground-water assessment atlas no. 2, part B, map 4. Montana Bureau of Mines and Geology, A Department of Montana Tech of The University of Montana, Butte, MT.
LaFave, J.I., Smith, L.N. & Patton, T.W. (2004) Ground-water resources of the Flathead Lake area: Flathead Lake Missoula, and Sanders Counties, Montana. Part A – descriptive overview and water-quality data. Montana Bureau of Mines and Geology, Butte, MT.
McMechan, R.D., & Price, R.A. (1980) Reappraisalof a reported unconformity in the Paleogene (Oligocene) Kishenehn Formation:Implications for Cenozoic tectonics in the Flathead Valley graben, southeasternBritish Columbia. *Bulletin of Canadian Petroleum Geology*, 28, 37–45.
Miller, H.G., & Singh, V. (1994) Potential field tilt – a new concept for location of potential field sources. *Journal of Applied Geophysics*, 32, 213–217.
Montana State Library (MSL) (2022) Montana Water Rights from the Montana Department of Natural Resources and Conservation Water Resources Division dates: 12/30/1845-02/17/2022. Downloadable data updated February 17, 2022 [accessed 9, March 2022]. https://msl.mt.gov/geoinfo/water_information_system/water_rights
Pirttijarvi, M. (2014) Markku's free software. https://sites.google.com/view/markkussoftware/home
Planert, M., & Williams, J.S. (1995) Groundwater atlas of the United States: segment 1, California, Nevada. United States Geological Survey hydrologic atlas 730-B, pp. B1–C28. https://doi.org/10.3133/ha730B.
Pugin, A.J.-M., Oldenborger, G.A., Cummings, D.I., Russell, H.A.J., & Sharpe, D.R. (2014) Architecture of buried valleys in glaciated Canadian Prairie regions based on high-resolution geophysical data. *Quaternary Science Reviews*, 86, 13–23.
Robson, S.G., & Banta, E.R. (1995) Groundwater atlas of the United States: segment 2, Arizona, Colorado, New Mexico, Utah. United States Geological Survey hydrologic atlas 730-C, pp. C1–C32. https://doi.org/10.3133/ha730C.
Rose, J. (2018) Three-dimensional hydrostratigraphic model of the subsurface geology, Flathead Valley, Kalispell, Montana. *Montana Bureau of Mines and Geology Open-File Report*, 703, 44.
Rose, J., Bobst, A., & Gebril, A. (2022) Hydrogeologic Investigation of the deep alluvial aquifer. Flathead Valley, Montana. Montana Bureau of Mines and Geology Report 32, p. 18.
Salem, A., & Ravat, D. (2003) A combined analytic signal and Euler method (AN-EUL) for automatic interpretation of magnetic data. *Geophysics*, 68, 1952–1961.
Salem, A. (2005) Interpretation of magnetic data using analytic signal derivatives. *Geophysical Prospecting*, 53(1), 75–82.
Schwartz, A. (1974) *Calculus and Analytic Geometry* (3rd ed). New York: Holt, Rinehart, and Winston.
Sharpe, D.R., Pugin, A.J.-M., & Russell, H.A.J. (2018) Geological framework of the Laurentian trough aquifer system, southern Ontario. *Canadian Journal of Earth Science*, 55, 677–708.
Smith, L.N. (2004a) Late Pleistocene stratigraphy and implications for deglaciation and subglacial processes of the Flathead Lobe of the Cordilleran Ice Sheet, Flathead Valley, Montana, USA. *Sedimentary Geology*, 165, 295–332.
Smith, L.N. (2004b) Surficial geologic map of the upper Flathead River valley (Kalispell valley) area, Flathead County, northwestern Montana: Montana Bureau of Mines and Geology Montana ground-water assessment atlas 2-B-06, 1 sheet, scale 1:70,000.
Smith, L.N. (2004c) Altitude of and depth to the bedrock surface: Flathead Lake Area, Flathead and Lake Counties, Montana: Montana Bureau of Mines and Geology Montana ground-water assessment atlas 2-B-07, 1 sheet, scale 1:150,000.
Smith, L.N. (2004d) Depth to deep alluvium of the deep aquifer in the Kalispell valley: Flathead County, Montana: Montana Bureau of Mines and Geology Montana ground-water assessment atlas 2-B-08, 1 sheet, scale 1:63,360.
Smith, L.N. (2004e) Thickness of the confining unit in the Kalispell valley, Flathead County, Montana: Montana Bureau of Mines and Geology Montana ground-water assessment atlas 2-B-09, 1 sheet, scale 1:100,000.
Smith, L.N. (2004f) Hydrogeologic framework of the southern part of the Flathead Lake Area, Flathead Lake Missoula, and Sanders counties, Montana: Montana Bureau of Mines and Geology Montana ground-water assessment atlas 2-B-10, 1 sheet, scale 1:300,000.
Smith, L.N. (2004g) Thickness of shallow alluvium, Flathead Lake Area, Flathead Lake Missoula, and Sanders counties, Montana: Montana Bureau of Mines and Geology Montana ground-water assessment Atlas 2-B-11, 1 sheet, scale 1:100,000.
Smith, L.N., Blood, L., & LaFave, J.I. (2000) Quaternary geology, geomorphology, and hydrogeology of the upper Flathead River valley area, Flathead County, Montana. In Roberts, Sheila, & Winston, Don (Eds.), *Geologic field trips, western Montana and adjacent areas: Rocky Mountain section of the Geological Society of America* (pp. 41–63). Missoula, MT: University of Montana.
Steuer, A., Siemon, B., & Auken, E. (2009) A comparison of helicopter-borne electromagnetics in frequency-and time-domain at Cuxhaven valley in North Germany. *Journal of Applied Geophysics*, 67, 194–205.

Stickney, M.C., Haller, K.M., & Machette, M.N. (2000) *Quaternary faults and seismicity in western Montana*. Special Publication no. 114. Butte, MT: Montana Bureau of Mines and Technology.

Tuma, J.J. (1979) *Engineering Mathematics Handbook* (2nd ed.). New York: McGraw-Hill.

U.S. Environmental Protection Agency. (2011) Summary of the groundwater system of the Flathead Lake basin. Public Review Draft. Helena, MT: U.S. Environmental Protection Agency, Montana Operations Office, p. 29.

United States Census Bureau. (n.d.). QuickFacts: Flathead County, Montana. [Accessed on June 10, 2023.] https://www.census.gov/quickfacts/flatheadcountymontana.

Van Kha, T., Vuong, H.V., Thanh, D.D, Quoc Hung, D., & Anh, L.D. (2018) Improving a maximum horizontal gradient algorithm to determine geological body boundaries and fault systems based on gravity data. *Journal of Applied Geophysics*, 152, 161–166

Verduzco, B., Fairhead, J.D., Green, C.M., & MacKenzie, C. (2004) New insights into magnetic derivatives for structural mapping. *The Leading Edge*, 23, 116–119.

Wijns, C., Perez, C., & Kowalczyk, P. (2005) Theta map: edge detection in magnetic data. *Geophysics*, 70 (4), 39–43.

Woollard, G.P. (1958) Results for gravity control network at airports in the United States. *Geophysics*, 28, 520–535.

WRCC. (2017) Kalispell Glacier AP, Montana (244558). [Accessed in March 2021.] http://www.wrcc.dri.edu/cgi-bin/cliMAIN.pl?mt4558.

Xue, G., Zhou, N., Guo, W., Fan, J., Lei, K., & Zhang, S. (2022) Delineation of sedimentary bauxite deposits in Shaanxi Province using the gravity and transient electromagnetic methods. *Ore Geology Reviews*, 144, 104865. https://doi.org/10.1016/j.oregeorev.2022.104865.

How to cite this article: Gebril, A., Khalil, M.A., Joeckel, R.M., & Rose, J. (2024) Analysis of legacy gravity data reveals sediment-filled troughs buried under Flathead Valley, Montana, USA. *Near Surface Geophysics*, 22, 402–417. https://doi.org/10.1002/nsg.12295